A Finite Element Analysis of the Fundão Dam Failure

Reza Moghaddam, Guillermo Riveros, Siavash Farhangi
Golder Associates, Mississauga, Ontario, Canada

ABSTRACT
The Fundão tailings dam failure of November 2015 in Brazil is one of the deadliest and most environmentally damaging tailings dam breaches in recent history. Roughly 32 million cubic meters (Mm3) of iron mine tailings were accidentally released in this catastrophic collapse, claiming the lives of nineteen villagers, and causing major environmental concerns after polluting local water systems. As part of the forensic investigation that followed, a finite difference analysis (FDA) simulation using the NorSand constitutive model in FLAC software was conducted by the Panel to test the hypothesis of lateral extrusion triggered failure. The purpose of the present study is to simulate the triggering of static liquefaction failure of the Fundão dam using a finite element analysis (FEA) approach in which the NorSand constitutive model is adopted in Rocscience RS2 software. A selected number of the Panel's laboratory test results were simulated in a series of FEA models to determine the validity of the numerical results and the strain-softening behaviour of the tailings. Drained triaxial compression tests were simulated to confirm calibration of the constitutive model. A computer model of the failing section of the dam's left abutment was subsequently generated for numerical analyses following the depositional details provided in the Panel's report. The results of the FEA are compared with the FDA shear stress-strain behaviour of the tailings reported by the Panel on a laboratory scale and for the dam's failing section, thus supporting the hypothesis of a slope failure triggered by a lateral extrusion mechanism. The implications and limitations associated with the FEA are further discussed in this paper.

RÉSUMÉ
La rupture du barrage Fundão en novembre 2015 au Brésil est une des ruptures plus meurtrières et plus dommageables pour l'environnement de l'histoire récente. Environ 32 millions de mètres cubes (Mm3) de résidus miniers de fer ont été accidentellement libérés lors de cet effondrement catastrophique, tuant dix-neuf villageois et causant de graves problèmes environnementaux après avoir pollué les systèmes d'eau locaux. Dans le cadre de l'enquête scientifique qui a suivi, une simulation numérique de l'analyse des différences finies (FDA) utilisant le modèle constitutif NorSand dans le logiciel FLAC a été menée par le Comité pour tester l'hypothèse d'une défaillance générée par l'extrusion latérale. Le but de la présente étude est de simuler le déclenchement de liquéfaction statique du barrage Fundão en utilisant une approche d'analyse par éléments finis (FEA) dans laquelle le modèle constitutif NorSand est adopté dans le logiciel Rocscience RS2. Une sélection de résultats d'essais en laboratoire du Comité a été simulés dans une série des modèles réalisés à base d'analyse FEA pour déterminer la validité des résultats numériques et aussi que la anti-écrouissage des résidus. Des essais de compression triaxiale drainée ont été simulés pour confirmer l'étalonnage du modèle constitutif. Un modèle de la section défaillante de la culée gauche du barrage a ensuite été généré pour des analyses numériques à la suite des détails de dépôt fournis dans le rapport du Comité. Les résultats de la FEA sont comparés au comportement contrainte-déformation de cisaillement de la FDA des résidus rapporté par le Panel à l'échelle du laboratoire et pour la section défaillante du barrage, soutenant ainsi l'hypothèse d'une rupture de pente déclenchée par une extrusion latérale. Les implications et les limites associées à la FEA sont discutées plus en détail dans cet article.

1 INTRODUCTION

The failure of the Fundão Dam in Brazil was undoubtedly a rude awakening to the mining and mine-waste management industries about the assumptions made during the design, construction, and maintenance of mining dams. After accidentally releasing roughly 32 million m3 of iron mine tailings on November 5, 2015, amounting to about 61% of the impoundment's contents, the breach buried the nearby town of Bento Rodrigues, claimed the lives of 19 villagers, and considerably polluted the local natural water systems.

Following the failure, a review panel (the Panel) was established to investigate the cause of the failure, issuing a report in August 2016 (e.g., Morgenstern et al. 2016). There have also been additional analyses of the Fundão Dam such as Riveros and Sadrekarimi (2019) and Reid (2019). For the purpose of this study, the approach adopted by the Panel (Morgenstern et al. 2016) was used to perform a series of deformation analyses on the failing section of the dam prior to its failure and to simulate the displacements reported to have triggered the static liquefaction failure of the dam. Conversely to the analysis using Fast Lagrangian Analysis of Continua (FLAC)

performed by the Panel, deformations are calculated in a series of four finite element analyses (FEA) in Rocscience RS2 software in this study. The first iteration consists of a relatively simple elastic analysis to determine the elastic deformations within the dam. The second iteration includes non-associated Mohr-Coulomb properties for all materials to evaluate the effect of yielding. Subsequently, with one iteration building on the Mohr-Coulomb model and another one on the elastic model, the third and fourth iterations include the critical state constitutive model NorSand (Jefferies 1993; Jeffries and Shuttle 2005) for the beached sand tailings in order to analyze the influence of state-dependent strength variations and yielding in the triggering of liquefaction. Lastly, to evaluate the implications associated with the FEA conducted in this study, the horizontal displacement results obtained are compared with those reported by the Panel in their base analyses.

2 FUNDÃO DAM FAILURE

2.1 History of the Fundão Dam

The Fundão Dam was the main containment structure in an iron tailings storage facility (TSF) built in the state of Minas Gerais, Brazil. Two types of slurry tailings (i.e., sand tailings and slimes) were produced because of the flotation concentration method used in iron mining (Vick 1990). The tailings were separately conveyed to the TSF. The sand tailings consisted of a mixture of sand-sized with finer silt particles that were free-draining, but susceptible to liquefaction when loose and saturated. The slimes, in contrast, were much finer and clay-like in nature with low permeability (Morgenstern et al. 2016).

The initial design of the embankment consisted of a compacted earth fill starter dam that was to be raised with an upstream configuration. The sands deposited upstream would in turn help retain water-borne slimes deposited separately farther upstream and prevent them from reaching the dam, as long as a minimum sand beach-distance of 200 m was maintained. Based on this initial design, saturation of the sands was to be prevented by a high-capacity drainage system built at the base of the starter dam that would allow the free-drainage of water from the deposited tailings.

A series of incidents beginning shortly after construction in 2009 required certain modifications to the initial plans and are believed to have promoted the eventual triggering of static liquefaction in the sand tailings. The first of these was the discovery of construction defects in the base drain, which forced the closure of the entire drainage system. The revised design made use of a blanket drain that was built on the surface of the sand tailings already contained inside the TSF, thus allowing the widespread saturation of the sands below. The second incident involved the mismanagement of the sand beach distance required to prevent slime deposits and water encroachment near the dam, which allowed slimes to settle in areas closer to the crest than originally designed. The third and last incident was the structural deficiency of a concrete conduit beneath the dam's left abutment, which was found incapable of sustaining any further loading generated by raising of the dam. Consequently, the dam's alignment was pushed upstream with the intent to reduce loading on the concrete conduit. This resulted in placing the crest directly over previously deposited slimes at the left abutment.

2.2 Panel's Dam Failure Conclusions

Following a thorough investigation into the probable causes of the breach, Morgenstern et al. (2016) concluded that failure was due to static (flow) liquefaction triggered in the left abutment where the necessary triggering conditions prevailed. The more compressible slimes that had encroached the sand beach area beneath the setback crest inhibited the free drainage required to control the phreatic surface, which in turn enhanced saturation of the loosely deposited sand tailings. The Panel hypothesized that lateral spreading of the slimes induced a drained relief of the effective mean stresses in the liquefiable sands at constant deviatoric stresses – a mechanism they termed "lateral extrusion," which ultimately led to the instability of the tailings sand matrix.

With the goal to assess the influence of slope deformations on the triggering of liquefaction at the Fundão Dam, the Panel carried out a set of deformation analyses on a cross-section through the region where the failure began. The deformation models were developed using FLAC finite difference software and simulated the staged construction of the dam in roughly four-month time intervals throughout most of its operational history. As previously described, three distinct analyses were performed: An analysis employing solely elastic material properties estimated from seismic cone penetration tests (SCPT); a Mohr-Coulomb analysis considering the strain-weakening response of the encroached slime layers; and a critical state analysis making use of the NorSand constitutive model to evaluate the effects of density-dependent shear strength and yielding. Their results showed that horizontal displacements were concentrated in two regions located at the interface of the sand tailings with the predominantly slime layer. With the largest horizontal deformations being in a region downstream of the dam crest, the Panel concluded that this was the most plausible location where liquefaction was triggered.

3 DEFORMATION ANALYSES MODEL PROPERTIES

FLAC utilizes an explicit finite difference formulation that can model complex behaviors, such as problems that consist of several stages, large displacements and strains, non-linear material behavior, or unstable systems. However, compared to the FE methods, FLAC analyses are generally time consuming and not routinely carried out in many geotechnical applications. As part of this study, the deformation analyses of the Fundão Dam left abutment were carried out with finite element (FE) method in Rocscience RS2 software. The base abutment analyses conducted by the Panel were emulated to the best extent possible, using the triggering of static liquefaction failure to draw comparisons of the results. This section describes both the development of the numerical model of the failing slope, including the material properties employed, and the series of deformation analyses conducted.

3.1 Fundão Tailings Deposition Cycle and Material Properties

The Panel's numerical model was developed to simulate the staged construction of the dam following the construction history from survey data and internal dyke stratigraphy. Despite thoroughly describing the methodology employed to define the spatial reconstruction of the abutment, public records of the investigation do not include clearly identifiable and scalable dyke profiles covering the complete timeline from March 2013 to November 2015 in the same 4-month intervals used in the development of the Panel's model. As a result of the limited amount of information available, a simple two-stage model was built for this study, covering the construction stages of the left abutment that occurred between August 2014 and November 2015. Owing to the unequal stage reconstruction timeline and understanding the effects this has on the absolute horizontal displacements produced, only the incremental displacements from the latter timeline are used in the comparison of the results.

Figure 1 shows the location of the section evaluated and the numerical model developed for the series of FEAs conducted.

The phreatic levels for each stage were based on piezometric data reported by the Panel, and zero and full saturation were respectively assumed above and below the piezometric lines. The material properties of each of the geotechnical units in the model are presented in Tables 1 and 2 for the three types of FEA conducted.

The materials identified are namely the compacted and deposited sand tailings; graded sand-slime mixtures consisting of predominantly slimes (100% slimes), mixed sand and slimes (50% slimes), interbedded slimes (20% slimes), and isolated slimes (100% sand); and bedrock. The layer of graded sand-slime mixtures represents the relative proportions of these materials that the Panel considered to be credibly present throughout the cross section based on deposition records and slimes mass balance analyses (Morgenstern et al. 2016). The unit weights of all materials were considered 22 kN/m^3. All material properties were obtained from the Panel's report, and their evaluation is briefly described in the following sections.

3.1.1 Elastic Properties

The large-strain elastic properties of the deposited sand tailings were estimated by the Panel from 2015 SCPT data through the beach of the dam by dividing the calculated small-strain shear modulus (G_{max}) values by a factor of 3. Similarly, the elastic properties of the slimes were empirically estimated from one-dimensional compression testing, and those for the sand-slimes mixtures were estimated as combinations based on their slimes-to-sand proportions. Whereas the elastic property inputs in the Panel's FLAC model were in the form of a bulk modulus, K, relationship as a function of effective vertical stress, σ'_{vc} (assuming a Poisson's ratio of 0.3), the FEA model in RS2 requires elastic inputs in the form of Young's modulus (E).

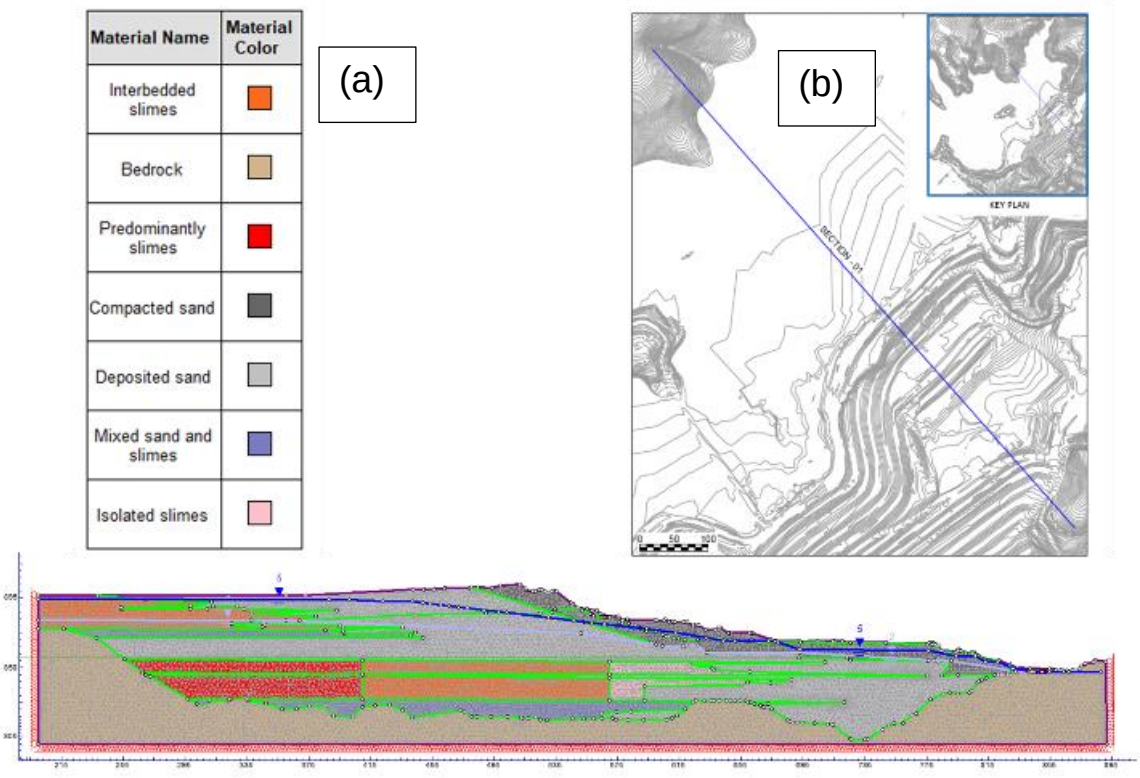

Figure 1. (a) FE model of the Fundão Dam's left abutment and (b) plan view

This relationship conversion was readily calculated from elastic theory principles for plain-strain boundary conditions.

Table 1. Summary of FEA Material Properties

Material	Elastic Properties[1]	Mohr-Coulomb Parameters
Compacted Sands	$E = 52\left(\frac{\sigma'_{vc}}{100}\right)^{0.4}$ MPa, E*=76 MPa, ν=0.3	ϕ'=35°, c'=5 kPa
Deposited Sands	$E = 52\left(\frac{\sigma'_{vc}}{100}\right)^{0.4}$ MPa, E*=100 MPa, ν=0.3	ϕ'=33°, c'=0 kPa
Predominantly slimes	$E = 9.4\left(\frac{\sigma'_{vc}}{100}\right)^{0.7}$ MPa, E*=18 MPa, ν=0.3	S_u/σ'_{vc}=0.22 (peak); S_u/σ'_{vc}=0.22 (residual)
Interbedded slimes	$E = 43.3\left(\frac{\sigma'_{vc}}{100}\right)^{0.42}$ MPa, E*=70 MPa, ν=0.3	S_u/σ'_{vc}=0.47 (peak); S_u/σ'_{vc}=0.47 (residual)
Isolated slimes	$E = 52\left(\frac{\sigma'_{vc}}{100}\right)^{0.4}$ MPa, E*=55 MPa, ν=0.3	S_u/σ'_{vc}=0.52 (peak); S_u/σ'_{vc}=0.52 (residual)
Mixed sand and slimes	$E = 30.4\left(\frac{\sigma'_{vc}}{100}\right)^{0.47}$ MPa, E*=75 MPa, ν=0.3	S_u/σ'_{vc}=0.39 (peak); S_u/σ'_{vc}=0.39 (residual)
Bedrock	E=500 MPa, ν=0.3	-

[1] E* values correspond to the 85th percentile of those calculated for the ranges of effective stress observed in the model

Table 2. Critical State Parameters

Material	NorSand Parameters
Deposited Sands	Γ=0.865, λ_e=0.024, M_{tc}=1.33, N=0.38, H_o=156, H_y=756, χ_{tc}=7.2

3.1.2 Mohr-Coulomb Parameters

For the Mohr-Coulomb model, the compacted sand Mohr-Coulomb parameters were obtained from the dam's original design (Morgenstern et al. 2016). In contrast, the deposited sand was modeled using the calculated critical state friction angle of φ' = 33° with c'=0 kPa, as established by the Panel from the triaxial compression tests completed as part of its investigation. Because the slimes and sand-slimes mixtures were conceptualized to mobilize undrained strength immediately after each loading increment, successively dissipating excess pore water pressures between loading stages, a combination of drained stiffness moduli and undrained shear strength was employed. While the Panel used a strain-weakening Mohr-Coulomb relationship involving peak undrained strength linearly reducing to residual values at 20% shear strain, the Mohr-Coulomb model in RS2 is an elasto-brittle-plastic material model, which means that the strength of the material instantly drops from its peak at initial yielding to the constant residual value thereafter. Since the brittle drop in shear strength was noticed to result in considerably larger displacements than those in the strain-weakening model, a simple elastic perfectly plastic model employing equal peak and residual undrained strength ratios was adopted for the analyses in this study.

An additional difference to the Panel analyses is that due to convergence challenges, constant values of E were employed, corresponding to the 85th-percentile of the stiffness values estimated for the range of σ'_{vc} observed. This percentile was selected to eliminate the otherwise weighing effect of the low E-values for σ'_{vc} < 100 kPa in the arithmetic mean, which would result in the underestimation of stiffness at higher depths.

3.1.3 NorSand Parameters and Calibration

The critical state constitutive model NorSand was used to evaluate the effects of state-dependent shear behavior of the deposited sand only. This particular constitutive model requires the input of several parameters associated with the critical state (Eq. 1), stress- and state-dilatancy relationships (Eq. 2 and 3, respectively), and plastic hardening (Eq. 4), all to be obtained from a comprehensive program comprised of laboratory testing and iterative numerical modelling.

$$e_{cs} = \Gamma - \lambda_e \ln \sigma'_m \quad [1]$$

$$\eta_{max} = D_{min}\mathrm{N} + M_{tc} \quad [2]$$

$$D_{min} = \chi_{tc}\psi_{D_{min}} \quad [3]$$

$$H = H_o - H_y\psi \quad [4]$$

e_{cs}: void ratio at critical state

Γ: reference void ratio on CSL

λ: slope of the critical state line (CSL) in e-ln(σ'_m) space

$\bar{\sigma}'_m$: mean effective stress (= p′ under triaxial conditions= $(\bar{\sigma}_1 + \bar{\sigma}_2 + \bar{\sigma}_3)/3$)

η: dimensionless shear measure as ratio of stress invariants $\eta = \bar{\sigma}_y/\bar{\sigma}_m$

D_{min}: maximum dilation rate (the subscript min reflects convention of positive compression)

N: volumetric coupling coefficient

M_{tc}: critical friction ratio in triaxial compression

χ_{tc}: dilatancy constant in triaxial compression

ψ : state parameter (=e_c – e_{cs})

H_o: plastic hardening modulus

H_y: change in hardening modulus with ψ

As part of its investigation, the Panel carried out extensive analyses to determine the NorSand parameters shown in Table 2. In addition to those, the Panel estimated the initial state parameter (ψ) for the analysis to equal -0.02 based on a series of numerical simulations to match the 80th percentile state parameter within the model, estimated from previous CPT investigations completed at the Fundão Dam. All the same parameters were used in this study; and as presented in Figure 2, finite element simulations of isotropically consolidated drained triaxial compression tests (IC-TxC) performed in RS2 exhibited relatively close fidelity to the laboratory test results (Figures 2a and 2b), as well as the Panel's NorSand simulations in FLAC (Figure 2a). Note that because liquefaction triggering was concluded by the Panel to have occurred under drained conditions, only drained triaxial tests were simulated here. Therefore, from the results observed, it was confirmed that the NorSand constitutive model in RS2 was capable of capturing the stress-strain relationship and volumetric response of the deposited sands appropriately.

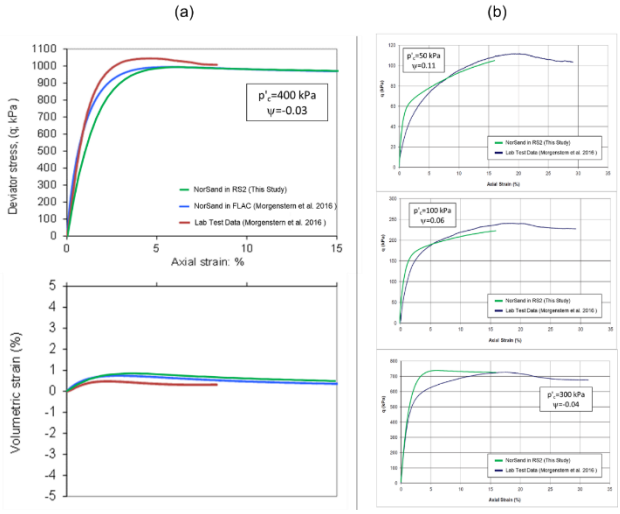

Figure 2. Comparison of the drained shearing behavior of Fundão sand tailings using (a) laboratory test data, and FEA and FLAC simulation results; and (b) laboratory test data and FEA results

4 DEFORMATION ANALYSES RESULTS

4.1 Elastic Analysis

The contours of the horizontal displacement obtained from the simple elastic FEA identified regions of concentrated lateral deformations, as shown in Figure 3a. These regions are located mostly in areas within and above the interbedded slimes layers, with the highest displacement magnitudes (highlighted in red) ranging from 60-70 mm in a region below and downstream from the dam crest. For comparison, the absolute horizontal displacement distribution obtained by the Panel is reproduced in Figure 3b, exhibiting similar contours as those obtained from the FEA. As explained by Morgenstern et al. (2016), "the upstream zone is a result of material settling above the highly compressible zone of predominantly slimes and sliding along the interface with the bedrock", while "the downstream zone is a result of the dam's geometry". However, it should be noted that the magnitudes shown for the Panel's results are different from those shown for this study due to the difference in stage reconstruction previously mentioned. As will be discussed later, a better comparison can be made by juxtaposing the incremental displacements from August 2014 to November 2015 reported by the Panel with those obtained here.

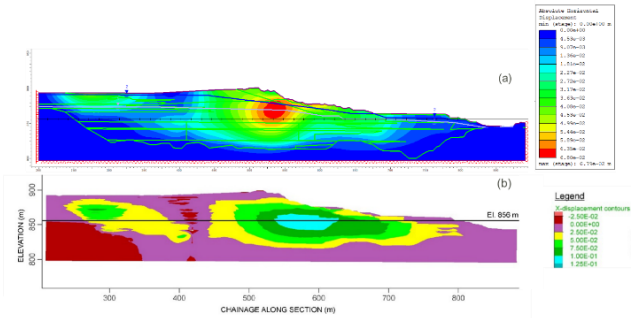

Figure 3. Comparison of horizontal displacement contours between the elastic (a) FEA and (b) FLAC (adapted from Morgenstern et al. 2016)

4.2 Mohr-Coulomb Analysis

The contours of the horizontal displacement from the Mohr-Coulomb FEA obtained in this study are shown in Figure 4a. As identified in the previous elastic analysis, regions of concentrated lateral deformations are located mostly in areas within and above the interbedded slimes layers. The highest displacements of 60-70 mm are still located in the region below and downstream from the dam crest. Comparably, the Panel's absolute horizontal displacement distribution, shown in Figure 4b, exhibits contours closely matching those obtained from the FEA. As mentioned before, however, the magnitudes shown for the Panel's results are different from those shown for this study as a result of the differences in stage reconstruction adopted.

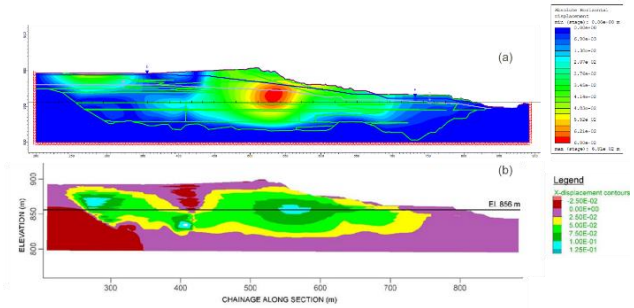

Figure 4. Comparison of horizontal displacement contours between the Mohr-Coulomb (a) FEA and (b) FLAC (adapted from Morgenstern et al. 2016)

4.3 Critical State Analysis

The critical state analysis employing the NorSand constitutive model was performed as an extension of the Mohr-Coulomb analysis in order to consider the dependency of the deposited sand's shear strength on its density – or more precisely, its state of stress (i.e. the state parameter). The contours of the horizontal displacement from this FEA are shown in Figure 5a. Broadly speaking, the distribution of concentrated lateral deformations is somewhat similar to those in the previous analyses. However, a slight upward shift of the region below and downstream from the dam crest is observed, while also exhibiting higher magnitudes of displacement (~122 mm). In the same manner, as shown in Figure 5b, the Panel's absolute horizontal displacement distribution shows contours generally comparable with those obtained from the FEA.

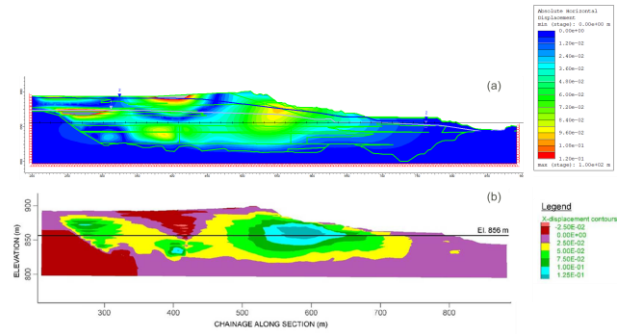

Figure 5. Comparison of horizontal displacement contours between the critical state (a) FEA and (b) FLAC (adapted from Morgenstern et al. 2016)

5 DISCUSSION OF RESULTS

In the absence of a common loading-stage reference profile between the simulations performed in this study and those by the Panel (i.e. the one 15-month stage in this study from August 2014 to November 2015 and the seven 4-month stages from March 2013 to November 2015), resulting from the limited amount of information publicly available, direct comparisons of the absolute horizontal displacement magnitudes were not feasible. For this reason, only the incremental changes in horizontal displacements from August 2014 to November 2015 reported by the Panel were extracted from the report and used for direct juxtaposition with the displacement results obtained here; thus using the dam profile from August 2014 as the zero-displacement reference.

Because the largest horizontal displacements were shown to concentrate in a zone that was beneath and downstream of the dam crest, centered approximately along El. 856 m, data in this section were used to compare the results. Figure 6 presents an assessment of the incremental horizontal displacements obtained in each of the FEA. These plots also include the accumulative horizontal displacements from the FLAC models used by the Panel for the period of August 2014 to November 2015. Altogether, consistent trends along the section can be observed with a few differences in magnitudes at specific sections as is discussed next.

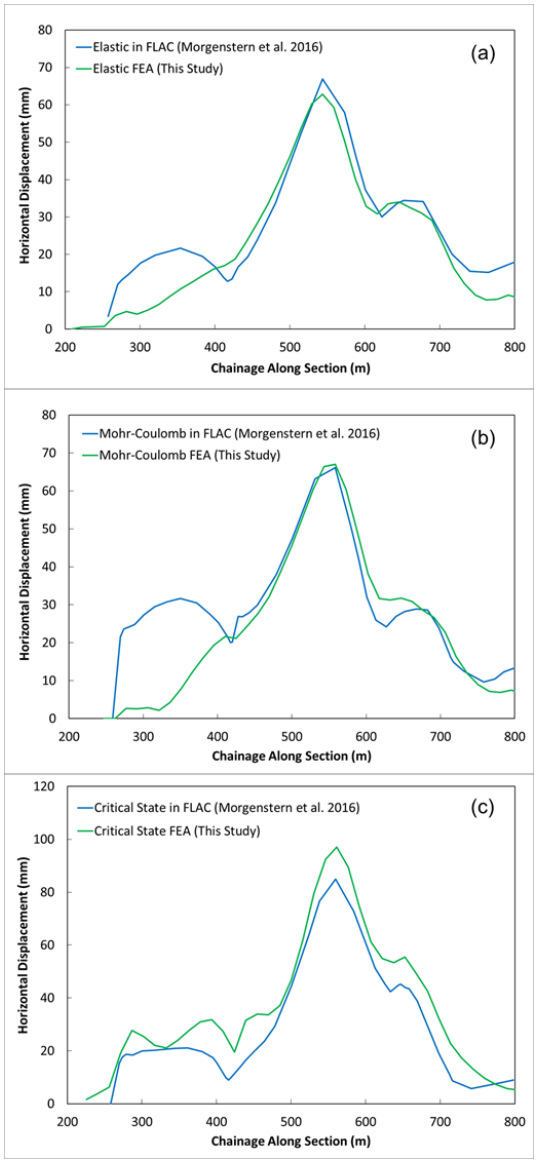

Figure 6. Comparisons of horizontal displacement trends at El. 856 m between FEA and FLAC for (a) elastic analyses, (b) Mohr-Coulomb analyses, and critical state analyses.

As shown in Figure 6a, the largest horizontal displacements in the elastic FEA occur in a region beneath and slightly downstream of the dam crest, at a chainage distance of approximately 540 m. With a magnitude of 63 mm, the maximum displacement obtained from the FEA compares well with that from the Panel's FLAC model (67 mm). In the downstream direction, both trends seem to follow each other up to a chainage distance of about 700 m, where they begin to steadily diverge, although still somewhat paralleling one another. This segment corresponds to a region of sands deposited on interbedded and isolated slimes. Differences between the square

discretization in FLAC and the 3-noded triangle meshing may have caused this slight variability. The trends are seen to follow one another very closely upstream of the peak up to a chainage distance of 425 m with a displacement difference of ~4 mm, in a region where the sands begin to overlie the zone of predominantly slimes. Beyond this point, the trends show entirely different tendencies and magnitudes, with the FEA generally exhibiting lower displacements than the FLAC analysis, with a maximum deviation of 14 mm. For reference, this corresponds to approximately 12% of the maximum absolute displacement reported by the Panel (118 mm) from its elastic analysis.

Despite the difference in elastic parameter input from the elastic FEA, the Mohr-Coulomb analysis shows very similar results between the displacements estimated here and those from the FLAC analysis.

As shown in Figure 6b, the largest horizontal displacements in the Mohr-Coulomb FEA also occur at a chainage distance of approximately 540 m with a magnitude of 67 mm, correlating properly with that from the FLAC analysis (66 mm). Furthermore, both trends seem to continue following each other, with a slightly higher deviation of ~7 mm at a distance of approximately 630 m, up to a chainage distance of about 730 m where they begin to diverge slightly. As before, and based on the results obtained, the parameters used in this segment of the cross-section seem to be relatively similar despite the difference in input mode – namely, the elastic perfectly plastic model with constant stiffness used in the FEA. Conversely to the elastic FEA, however, both trends are observed to continue following each other very closely in the segment upstream of the peak displacement, up to a chainage distance of 425 m, with a maximum displacement difference of ~7 mm where the sands begin to overlie the zone of predominantly slimes. Once again, the trends show entirely different tendencies and magnitudes past this point, with the FEA exhibiting much lower horizontal displacements than the FLAC analysis. As a reference, the maximum deviation of 27 mm in this region corresponds to approximately 25% of the maximum absolute horizontal displacement reported by the Panel (106 mm).

This disparity of results is plausibly due to the axiomatic effect in material stiffness produced by the buildup of effective stress induced by an increasing overburden. In other words, volumetric strains are not only affected by the confining effective stresses applied, but also by the changes in void ratio produced with each loading/unloading cycle. Consequently, it seems reasonable that, since the E-σ'_{vc} relationship could not be successfully implemented, the constant stiffness values assigned in the FEA may have been overestimated in the zone of predominantly slimes, resulting in the smaller horizontal displacement obtained.

Lastly, Figure 6c presents the results of the critical state FEA. As shown in the graph, the largest horizontal displacements occur at a chainage distance of approximately 560 m, consistent with the slight shift of the concentrated region of displacements beneath the dam crest observed in both the FEA and the FLAC analysis shown in Figure 5. Unlike the two previous FEAs, the horizontal displacement trend in the critical state FEA is observed to parallel that of the FLAC analysis for the entirety of the section, including the segment overlying the zone of predominantly slimes. However, there seems to be a rather consistent offset in magnitude ranging from 10-15 mm, with the FEA yielding the upper values. For reference, this is equivalent to approximately 7-11% of the maximum absolute horizontal displacement reported by the Panel (135 mm) in its critical state analysis.

To investigate this issue further, a new critical state FEA was performed, coupling the NorSand constitutive model for the deposited sands with simple elastic models for all other materials rather than the Mohr-Coulomb models. As shown in Figures 7a and 7b, the contours and displacement magnitudes are more analogous to those of the Panel's FLAC model, despite exhibiting moderately smaller values. With a magnitude of 79 mm, the maximum displacement obtained from the modified critical FEA is now 6 mm lower than that from the FLAC analysis. In the downstream direction from the peak values, both trends seem to follow each other very closely. Likewise, both trends are observed to begin diverging slightly while still paralleling one another upstream of the peak displacements, up to a chainage distance of 450 m. Although the trends do not exactly replicate one another beyond this point, the leading tendency of horizontal displacements of 20 mm in magnitude is approached by this modified critical state FEA. Thus, these new results suggest that the yielding produced in the Mohr-Coulomb materials in the first critical state FEA (Figure 8) is the reason the horizontal displacements were initially overestimated.

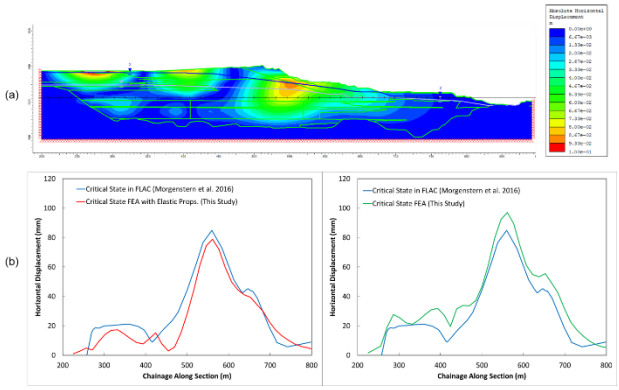

Figure 7. (a) Contours of horizontal displacement obtained from the critical state FEA employing NorSand for the deposited sands and elastic material properties for all other deposited materials; (b) comparisons of the horizontal displacement trends at El. 856 m between FEA and FLAC for the modified (left) and the initial (right) critical state analyses.

6 CONCLUSIONS AND LIMITATIONS OBSERVED

Finite element simulations were performed on the failing section of the Fundão Dam. These analyses paralleled the approach followed by the investigation Panel using FLAC in its evaluation of the deformations that caused the triggering of static liquefaction failure. The methodology adopted consisted of a series of elastic, Mohr-Coulomb, and critical state FEA deformation analyses.

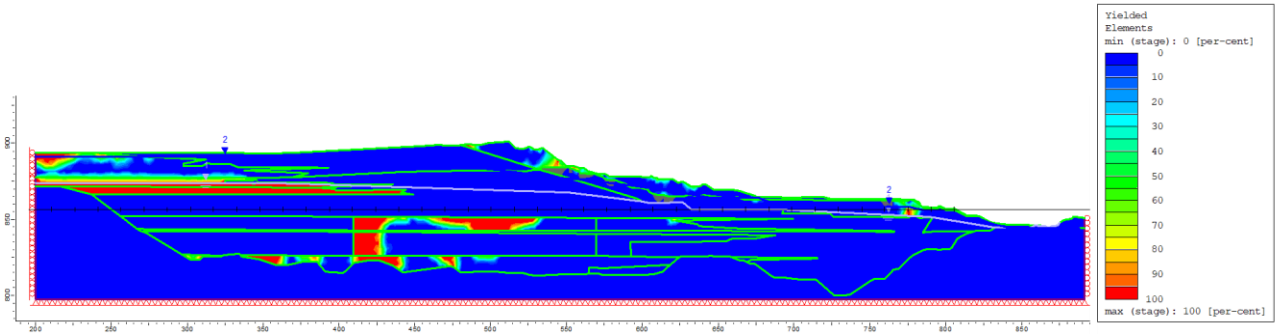

Figure 8. Contours of the yielded regions of initial FEA

For the most part, the FEA results exhibited regions of concentrated horizontal displacements upstream and downstream of the crest similar to those produced by the Panel's FLAC models. Furthermore, the trends of horizontal displacements at El. 856 m were observed to largely replicate the Panel's results, albeit two appreciable differences. The use of the relationship of E as a function of σ' in the FEA produced convergence issues when used in combination with Mohr-Coulomb parameters. As a result of this limitation, and despite giving acceptable results for the deposited sands and similar materials, the use of a constant Young's modulus in the elastic and Mohr-Coulomb FEAs for the regions of predominantly slimes produced considerable deviations in horizontal displacement near these zones when compared with those obtained from FLAC. Another observation is that yielding in the Mohr-Coulomb materials produced horizontal displacements 10-15 mm larger in magnitude than the Panel's results in the critical state FEA despite following the same overall tendencies. Notwithstanding these few limitations, and considering the scale of the deviations obtained with respect to the absolute displacements reported by the Panel, this series of FEA was able to adequately replicate the deformations and regions of critically-stressed tailings sands concentrating in the area beneath and downstream of the dam crest. Thus, it can be conjectured, in agreement with the Panel's conclusion, that this is the region where liquefaction would most likely have initiated.

7 REFERENCES

Galindo da Fonseca, P., and Galindo da Fonseca, I. (2016). *Brazil's Greatest Environmental Catastrophe – Samarco's Fundão Tailings Dam*. Environmental Policy and Law, 46/5: 334-337.

Morgenstern, N., Vick, S. G., Viotti, C. B. and Watts, B. D., 2016. *Report on the Immediate Causes of the Failure of the Fundão Dam*, Gottlieb Steen and Hamilton LLP.

Riveros, G.A., & Sadrekarimi, A. (2019). Static liquefaction analysis of the Fundão dam failure. *Proceedings of the ICOLD 2019 Symposium*, (ICOLD 2019)/ Publications du symposium CIGB 2019. Ottawa, Canada.

Vick, S. G. (1990). *Planning, Design, and Analysis of Tailings Dams*. John Wiley and Sons.

Jefferies, M G (1993). Nor-Sand: a simple critical state model for sand. GeotechniqueV43, N1, March 1993, P91–103. *International Journal of Rock Mechanics and Mining Sciences and Geomechanics Abstracts*, 30(5), 276–276.https://doi.org/10.1016/0148-9062(93)92281-T.

Jefferies, M.G., & Shuttle, D.A. (2005). NorSand: features, calibration, and use. In Soil constitutive models: evaluation, selection, and calibration. Edited by J.A. Yamamuro and V.N. Kaliakin. *ASCE Geotechnical Special Publication* 128, pp. 204–236.

Reid, D. (2019). Additional Analyses of the Fundão Tailings Storage Facility: In Situ State and Triggering Conditions. *Journal of Geotechnical and Geoenvironmental Engineering*. 2019, 145(11): 04019088 ASCE, ISSN 1090-0241.

8 ACKNOWLEDGEMENT

The authors thank Dr. Joe Carvalho (Golder Associated Ltd.) for providing numerical analysis technical support.